

AperTO - Archivio Istituzionale Open Access dell'Università di Torino

Shedding light on precursor and thermal treatment effects on the nanostructure of electrospun TiO₂ fibers

This is the author's manuscript

Original Citation:

Availability:

This version is available <http://hdl.handle.net/2318/1603061> since 2016-10-17T13:04:44Z

Published version:

DOI:10.1016/j.nanoso.2016.05.003

Terms of use:

Open Access

Anyone can freely access the full text of works made available as "Open Access". Works made available under a Creative Commons license can be used according to the terms and conditions of said license. Use of all other works requires consent of the right holder (author or publisher) if not exempted from copyright protection by the applicable law.

(Article begins on next page)

This Accepted Author Manuscript (AAM) is copyrighted and published by Elsevier. It is posted here by agreement between Elsevier and the University of Turin. Changes resulting from the publishing process - such as editing, corrections, structural formatting and other quality control mechanisms may not be reflected in this version of the text. The definitive version of the text was subsequently published in NanoStructures & NanoObjects 7 (2016) 495

You may download, copy and otherwise use the AAM for noncommercial purposes provided that your license is limited by the following restrictions:

(1) You may use this AAM for noncommercial purposes only under the terms of the BY-NC-ND license.

(2) The integrity of the work and identification of the author, copyright owner, and publisher must be preserved in any copy.

(3) You must attribute this AAM in the following format: Creative Commons BY-NC-ND license (<http://creativecommons.org/licenses/by-nd/4.0/deed.en>), <http://dx.doi.org/10.1016/j.nanos.2016.05.003>

Shedding light on precursor and thermal treatment effects on the nanostructure
of electrospun TiO_2 fibers

Sara Morandi, Claudio Cecone, Giulia Marchisi, Pierangiola Bracco, Marco Zanetti and Maela
Manzoli*

Dipartimento di Chimica, Università di Torino and NIS, Interdepartmental Centre, Via P. Giuria 7,
10125 Torino, Italy.

*Corresponding author: Dr. Maela Manzoli, phone: +390116707541, -mail:
maela.manzoli@unito.it

Abstract

Electrospinning technique was employed for the synthesis of TiO_2 samples, starting from titanium oxysulfate and titanium n-butoxide (TNBT) as precursors. The electrospun fibers, obtained after optimization of starting solutions, were either calcined in air at 450 °C or treated in 50 mbar of pure oxygen at 450 °C. The main goal was to obtain fibers constituted by crystallites with size lower than 10 nm (size largely reported in literature for this kind of synthesis) in the anatase form. Before thermal treatment, the morphology of the fibers was characterized by Scanning Electron Microscopy (SEM); after thermal treatment morphological and structural properties were determined by Transmission Electron Microscopy (TEM) as well as by high resolution TEM and X-Ray Diffraction (XRD).

TiO_2 prepared with TNBT precursor and treated in oxygen at 450 °C gave the best results in terms of crystalline phase (pure anatase) and particle size (about 5 nm). Moreover, analysis of the fibers obtained from TNBT before thermal treatment revealed that the precursor crystallization occurred already at room temperature during the electrospinning process, giving rise to nucleation germs for the subsequent growth of TiO_2 crystallites during the thermal treatment. On the contrary, samples prepared by electrospinning and by simple solvent evaporation at room temperature of the solution with the same TNBT precursor did not give the same promising results in terms of crystalline phase and particle size.

Keywords: Electrospinning, titanium oxysulfate, titanium n-butoxide, TiO_2 , HR-TEM

1. Introduction

Titanium dioxide (TiO₂) is a versatile transition metal oxide widely investigated as a useful material in a wide range of applications including solar cells [1,2], photocatalysts for air and water purification [3-5], gas sensors [6-8] and biocompatible coatings for biomaterials [9, 10]. The most common crystalline forms of TiO₂ are anatase and rutile, both showing a tetragonal crystalline structure. For the solar cell and photocatalysis applications, only the anatase TiO₂ exhibits high activity. However, the high rate of recombination of photo-induced electron and hole pairs limits its photo-activity, which strongly depends on physicochemical parameters such as particle size and surface area as well as overall morphology. To further improve properties of TiO₂ and to expand potential applications, low-dimensional nanostructures with controllable crystalline phases, such as nanoparticles, nanofibers, nanostructured thin films or coatings and nanotubes have been extensively studied. In particular, TiO₂ microtubes constituted by defined nanoscale particles have attracted considerable attention [11-16].

Electrospinning represents a relatively simple and versatile method for generating porous fiber mats with interconnective pores and high specific area [17]. In a typical process, a polymer solution or melt is injected from a small nozzle under the influence of an electric field as strong as several kV/cm. The built up of electrostatic charges on the surface of a liquid droplet induces the formation of a jet, which is subsequently stretched to form a continuous ultrathin fiber. In the continuous feeding mode, numerous copies of fibers can be formed within a period of time as short as a few seconds.

Until the early 2000s, electrospinning was mainly applied to pure organic polymers. In the last fifteen years, electrospinning of solutions containing precursors of ceramics followed by high temperature pyrolysis was adopted to obtain ceramic nanofibers [18-21]. In particular, in the last

few years, electrospinning synthesis of titania have demonstrated that the fibers obtained after calcination are polycrystalline with crystallite size in the range 50 nm [12, 13, 15, 225].

In the present work, different precursors and different thermal treatments on electrospun fibers were tested to obtain polycrystalline TiO_2 fibers with crystallite size lower than 10 nm in the anatase form. Before thermal treatment, the morphology of fibers was characterized by Scanning Electron Microscopy (SEM); after thermal treatment morphological and structural properties were determined by Transmission Electron Microscopy (TEM) and High Resolution Transmission Electron Microscopy (HRTEM) as well as by X-Ray Diffraction (XRD).

2. Experimental

2.1. Synthesis of the samples

Solutions for electrospinning were prepared using titanium(IV) oxysulfate (TiOSO_4 , Sigma Aldrich) or titanium (IV) n-butoxide (TNBT, Sigma Aldrich) as precursors. In the first case, an aqueous solution containing polyvinylpyrrolidone (PVP, 1300000 uma, Sigma Aldrich) and TiOSO_4 precursor was prepared and loaded into a syringe equipped with a BD Precisionglige needle (size 27 gauge) made of stainless steel and connected to a high voltage supply (GLASSMAN High Voltage, EL) capable of generating DC voltage up to 30 kV. As-electrospun fibers were collected on a drum collector (length: 120 mm, diameter: 60 mm), covered with an aluminum foil. During electrospinning a positive voltage of 30 kV was applied between the needle and the collector with a working distance of 14 cm. The feeding rate for the polymer precursor solution was controlled using a syringe pump (Biological Instruments, KD Scientific) and was set at 0.1 min. The electrospinning process was conducted in air at room temperature (PVP) and TiOSO_4 concentrations were optimized in order to obtain well defined fibrous structure as evidenced by SEM analysis (vide infra). Based on the results of a previous screening, PVP concentrations

between 13 and 25% and PVP/TiOSO₄ weight ratio ranging between 2/1 and 3/1 were tested and reported in Table 1.

Table 1. List of the solutions used for the optimization of the electrospinning process with TiOSO₄ precursor

| Solution n° | 1 | 2 | 3 | 4 | 5 | 6 | 7 |
|------------------------------|-----|-------|-----|-----|-----|-----|-----|
| PVP wt. % | 13 | 14 | 15 | 18 | 20 | 22 | 25 |
| PVP/TiOSO ₄ (w/w) | 2/1 | 2.5/1 | 3/1 | 3/1 | 3/1 | 3/1 | 3/1 |

As for the TNBT precursor, a solution was prepared by mixing two parts of ethanol, one part of TNBT and two parts of acetic acid, which is added to the solution by controlling the hydrolysis reactions of the gel precursor [11, 26]. A second solution with PVP (130000 uma) in ethanol was prepared. Also in this case the PVP concentration was optimized by checking the solutions reported in Table 2 in order to obtain well defined fibrous structure as evidenced by SEM analysis (vide infra).

Table 2. List of the solutions used for the optimization of the electrospinning process with TNBT precursor

| Solution n° | 1 | 2 | 3 | 4 | 5 |
|-------------|---|----|----|----|----|
| PVP wt. % | 7 | 10 | 15 | 18 | 20 |

Equal volumes of the two solutions were mixed just before the loading in the syringe for the electrospinning process, in air, at RT with a feeding rate of 0.1 ml/min, a voltage of 30 kV and a working distance of 14 mm.

For each precursor only the sample with the best fiber morphology underwent two different thermal treatments to burn the organic component: (i) calcination in air at 450 °C for 3 hours; (ii) thermal treatment in 50 mbar of pure oxygen at 450 °C for 5 h, changing oxygen every hour. In this way four TiO₂ samples were prepared: two with TiOSO₄ precursor, named TiOS_{air} (calcination in air) and TiOSO_x (thermal treatment in O₂) and two with TNBT precursor, named TNBT_{air} (calcination in air) and TNBT_{O₂} (thermal treatment in O₂).

For comparison purposes, the solution containing TNBT precursor was also used for preparing samples by electrospray technique and by simple evaporation of the solvent at RT. To prepare the sample by electrospray technique the same apparatus employed for the electrospinning procedure was used. In this case, PVP with a lower molecular weight (30000 uma) was used in order to obtain droplets instead of fibers.

2.2. Characterization techniques

Thermogravimetric analysis (TGA) of the electrospun samples was performed by a TGA Q500 TAInstrument, using a temperature ramp of 10 °C/min up to 800 °C in air.

Morphological characterization of the samples was performed by: (i) Scanning Electron Microscopy (SEM) using a Leica Stereoscan 410 microscope (Oxford Instruments), operating at 15 kV. All the polymercontaining samples were gold sputtered prior to examination; (ii) Transmission Electron Microscopy (TEM) and High Resolution (HRTEM) using a side entry Jeol JEM 3010 (300 kV) microscope equipped with a LaB₆ filament. For analyses, if not differently specified, the synthesized samples were deposited on a copper grid, coated with a porous carbon film. All digital micrographs were acquired by an Ultrascan 1000 camera and the images were processed by digital micrograph. A statistically representative number of crystallites was counted in order to obtain the particle size distribution where the mean particle diameter, \bar{d} , was calculated as $\bar{d} = \sum d_i n_i / \sum n_i$, where n_i was the number of particles of diameter d_i .

Structural characterization of the samples after thermal treatment was carried out on a Oxford Diffraction Gemini-R Ultra diffractometer (Cu-K, radiation, $\lambda = 1.5418 \text{ \AA}$) equipped with an Enhanced Ultra collimator, a four-circle Kappa geometry goniometer and a RUBY CCD collector. This instrument, suitable for XRD measurement on single crystals, was adapted to work with powders: the advantage is the very low amount of sample necessary for a measurement. The crystallite size of TiO₂ was calculated by applying the Scherrer's formula using the (101) diffraction peak for anatase and the (110) diffraction peak for rutile in the XRD patterns.

3. Results and Discussion

3.1 Fiber synthesis optimization

The purpose of this work has been to use a polymer as template for the production of titania nanoparticles. With this aim we selected PVP as the base polymer because of its good solubility in alcohols and water and because of its compatibility with both organic and inorganic titania precursors even when its molecular weight is as high as 130000.

In Figure 1 SEM images of the as prepared samples obtained by electrospinning of solutions with TiOSO_4 precursor are shown. Solutions 1, 2 and 3 (see Table 1) give the same morphology, which is reported in Fig.1A for solution 2: an high amount of beads is observed, indicating a too low solution viscosity. Images in section B and C related to the electrospinning of solutions 4 and 5, respectively, show the presence of quite defined fibers, even if some fiber adhesion is still present. Solutions 6 and 7 allow to obtain well defined fibers as reported in image of section D for solution 7. This last sample was chosen for the subsequent thermal treatments in air and oxygen at 450 °C for obtaining TiO_2 specimens.

In Figure 2 SEM images of the as prepared samples obtained by electrospinning of solutions with TNBT precursor are shown. The results obtained with solutions 1 and 2 (see Table 2) is the same and is reported in section A for solution 2: the presence of beads enlightens the too low viscosity of the solution. The increase of PVP concentration increases the solution viscosity, causing the decrease of beads amount with solution 3 (image in section B) and disappearance with solutions 4 and 5 (see image in section C related to solution 5). The sample with well defined fibers obtained with solution 5 was chosen for the subsequent thermal treatments.

It is worth of note that with TiOSO_4 precursor the best obtained fibers (Fig. 1D) are wider (the diameters have size in the range between 0.5 and 7.0 μm) than in the case of TNBT precursor,

that guaranteed fibers with homogeneous diameter $< 1 \mu\text{m}$ (Fig. 2C). This is likely due to differences in viscosity and conductivity between the two precursor solutions.

The TG analysis performed in air on the two samples chosen for undergoing thermal treatments shows that for both of them the weight loss associated to the polymer volatilization ends at about 450 °C (Figure 3). For this reason, the temperature of 450 °C was chosen for carrying out calcination and thermal treatment in 50 mbar of pure oxygen.

3.2 Characterization of TiO₂ samples obtained by electrospinning

After thermal treatments four samples were obtained: TiOSair, TiOSOx, TNBTair and TNBTOx, whose diffraction patterns are reported in Figure 4. TiOSair is constituted mainly by anatase with small amount of rutile phase (curve a). The mean crystallite size of anatase is calculated to be about 11 nm. The diffraction pattern of TiOSOx (curve b) reveals a very low crystallinity of the sample with the presence of a very broad and weak peak at 25.3° related to the main (101) reflection of anatase. Moreover, at angles lower than 20° a very broad peak assignable to amorphous phase is detected. As a matter of fact, the TiOSOx sample appears black, revealing the presence of a significant amount of carbonaceous residues. This result puts in evidence that thermal treatment at 450 °C with low Q pressure is not sufficient to efficiently burn the organic component when using TiOSO₄ as precursor. With thermal treatments in pure oxygen at higher temperatures a relevant amount of rutile is obtained. This phase is undesired for photocatalysis and solar cell applications.

As for samples prepared with TNBT precursor, the diffraction pattern of TNBTair (Fig. 4, curve c) shows the presence of both anatase and rutile phases. The mean crystallite size of anatase (using the (101) peak at 25.3°) and rutile (using the (110) peak at 27.4°) is calculated to be about 11 and 14 nm, respectively. The pattern of TNBTOx (Fig. 4, curve d) reveals a particularly interesting sample, constituted by only anatase with a mean crystallite size of about 5 nm.

TEM and HRTEM measurements were performed on this last sample and two representative images are reported in Figure 5 sections A and B. The images reveal that the fibrous nature of the sample is maintained after the thermal treatment even if the fibers appear fragmented due to the lower mechanical resistance of the oxide with respect to the electrospun material. The analysis of the fiber diameter distribution, obtained by sampling 54 fibers, is reported in Figure 6A: the range of fiber diameter is 32-230 nm with a mean value of 79.0 nm and a standard deviation of 50.2 nm, evidencing the presence of fibers with different diameter. However, it is well evident that the TiO₂ fibers are constituted by nanoparticles whose crystalline nature is enlightened by diffraction fringes present in the HRTEM image (Figure 5B) and by diffraction spots in the Fourier Transform of the image (Figure 5C). The analysis put in evidence spacings of 3.52, 2.37 and 1.88 nm related to the (101), (103) and (200) planes of tetragonal anatase (ICDD 001-0562).

Particle size distribution, obtained by sampling 250 particles, is reported in Figure 6B. The sample is highly homogeneous, being the size distribution narrow with an average diameter of 54 nm and a standard deviation of 1.1 nm, in full agreement with the results obtained on the basis of the XRD pattern.

It is worth of note that differently from the case of TiOSO₄, the thermal treatment in low oxygen pressure of the sample obtained from TNBT precursor allows to burn all the organic fraction already at 450 °C, obtaining pure anatase with particularly small particle sizes. Indeed, PVP is thermally degraded, predominantly, by the release of the pyrrolidone side group and the subsequent decomposition of polyenic sequences [27]. In inert atmosphere those polyenic sequences, undergoing to condensation reaction, may lead to the formation of a certain amount of carbonaceous residue. However, if the degradation is carried out in the presence of oxygen the residue volatilizes completely through a thermoxidative mechanism. Results show that this reaction occurs obviously in the case of TiO₂Air and TNBTair, where the amount of oxygen is sufficient to produce the complete volatilization of the organic fraction at 450 °C. This also happens in the case of TNBT_x, where despite the low partial pressure of O₂ the volatilization of the

organic phase is complete. However, in the case of TiO_2 , the formation of a carbonaceous residue prevails. It must be considered that organic salts and acids are known to increase the char yields of degrading polymers, promoting dehydration reactions [28]. The presence of an acid salt like TiOSO_4 may enhance the formation of char at the point that it is impossible to be thermally oxidized in the low-pressure condition employed.

In order to deepen the comprehension of the mechanism for the formation of TiO_2 particles, HR-TEM analysis of the fibers before the thermal treatment was performed. For this purpose, fiber deposition was performed directly on a TEM copper grid. In Figure 7 an image of the not calcined fibers directly electrospun on the grid is shown. The related Fourier Transform is also reported as inset. Even if the sample has mainly an amorphous nature, some crystalline regions are present confirmed by the spots detected in the Fourier Transform of the acquired images. The distances of these spots from the transmitted beam can be related to stoichiometric TiO_2 phases, such as Ti_2O_3 (JCPDS 0010-0063), Ti_3O_5 (JCPDS 0011-0217) and Ti_7O_{13} (JCPDS 0018-1403). It is necessary to underline that the sample is stable under electron beam, excluding the hypothesis of the formation of stoichiometric TiO_2 phases during the HRTEM analysis. This finding is of pivotal importance because evidence that the precursor crystallization occurs already at RT during the electrospinning process is given. The early crystallization can provide nucleation germs for the subsequent growth of TiO_2 crystallites during the thermal treatment in oxygen. This phenomenon, which is generally not observed when using other preparation techniques, might be favored by the stretching effect to which the precursor solution is usually subjected during electrospinning. Reasonably, the formation of high amount of nucleation germs, as evidenced by HR-TEM measurements, along with low oxygen pressure can justify the formation of particles smaller than those obtained in the other cases under study.

3.3 Samples prepared by electrospray and solvent evaporation

In order to demonstrate the uniqueness of the electrospinning technique for obtaining TiO_2 with very small crystallite size in anatase form, other two samples were prepared by electrospray technique and by simple solvent evaporation at RT using the solution 5 of Table 1. It should be considered that in order to obtain droplets with electrospray, a lower molecular weight PVP (30.000 uma) was employed. In Figure 8 SEM image of the sample prepared by electrospray is reported, evidencing the formation of droplets in a wide range of diameters (0.12 μm).

The samples prepared by electrospray and solvent evaporation were treated at 450 °C in 50 mbar of oxygen, i.e. the thermal treatment that allowed to obtain the best TiO_2 sample in terms of crystalline phase (pure anatase) and particle size (about 5 nm) by electrospinning. However, for these two samples the thermal treatment was not sufficient to burn the entire organic fraction. In the last two cases, the samples have a lower specific area rendering more difficult the oxidation process, as much of the organic fraction to be ablate is located in the bulk in which the oxygen must diffuse. In order to obtain white sample, it was necessary to treat the electrospray sample at 650 °C and that obtained by simple solvent evaporation at 700 °C. This causes the formation of high amount of rutile phase with crystallite size of about 20 nm, as evidenced by XRD patterns reported in Figure 9.

4. Conclusions

In the present work, polycrystalline TiO_2 fibers were synthesized through electrospinning technique. In particular, titanium(IV) oxysulfate (TiOSO_4) and titanium(IV) n-butoxide (TNBT) were used as precursors along with polyvinylpyrrolidone (PVP) for preparing solutions for electrospinning. Precursors and PVP concentrations were optimized to obtain well defined fibers.

Both calcination in air and thermal treatment in 50 mbar of pure oxygen at 450 °C were performed for obtaining TiO_2 samples.

Among the synthesized TiO_2 samples, that prepared with TNBT precursor and treated in low oxygen pressure at 450 °C gives the best results in terms of crystalline phase and particle size: XRD

pattern shows the presence of only anatase with a mean crystallite size of about 5 nm, in agreement with HR-TEM measurements. In particular, HRTEM analysis of the fibers obtained from TNBT before thermal treatment puts in evidence that the precursor crystallization occurs already at RT during the electrospinning process, giving nucleation germs for the subsequent growth of TiO₂ crystallites during the thermal treatment. It is worth of note that the treatment in low oxygen pressure along with the formation of a high amount of nucleation germs allows to obtain particles smaller than those obtained in the other cases under study.

The results obtained on samples prepared by electrospinning were compared with those collected on samples synthesized by electro spray technique and by simple solvent evaporation at RT using TNBT precursor and thermal treatment in low oxygen pressure. The need of electrospinning technique for obtaining TiO₂ with very small crystallite size in anatase form was demonstrated. As a matter of fact, for samples obtained by electro spray and solvent evaporation the organic fraction was burn only at 650 °C, producing TiO₂ with high amount of rutile phase and crystallite size of about 20 nm.

References

- [1] R. Bendoni, N. Sangiorgi, A. Sangiorgi, A. Sanson, Role of water in TiO₂ spinning inks for dyesensitized solar cells, *Sol. Energy* 122 (2015) 407.
- [2] P. Yang, Q. Tang, A nanoporous titanium dioxide framework for dye sensitized solar cell, *Mater. Lett.* 161 (2015) 1858.
- [3] T. Ochiai, S. Tago, M. Hayashi, H. Tawarayama, T. Hasegawa, A. Fujishima, TiO₂ Impregnated porous silica tube and its application for compact air water purification units, *Catalysts* 5(3) (2015) 1496.

- [4] M. Roso, A. Lorenzetti, C. Boaretti, D. Hrelja, M. Mestri, Graphene/TiO₂ based photo catalysts on nanostructured membranes as a potential active filter media for methanol gas degradation, *Appl. Catal. B: Env.* 176 (2015) 225-232.
- [5] S.W. Verbruggen, TiO₂ photocatalysis for the degradation of pollutants in gas phase: From morphological design to plasmonic enhancement, *J. Photochem. Photobiol. C: Photochem. Rev.* 24 (2015) 6482.
- [6] Z.-p. Yang, X. Liu, C.-j. Zhang, B.-z. Liu, A high-performance nonenzymatic piezoelectric sensor based on molecularly imprinted transparent TiO₂ film for detection of urea, *Biosens. Bioelectron.* 74 (2015) 890.
- [7] W. Guo, Q. Feng, Y. Tao, L. Zheng, Z. Han, Ma, Systematic investigation on the gas sensing performance of TiO₂ nanoplate sensors for enhanced detection on toxic gases, *Mater. Res. Bulletin* 73 (2016) 302-307.
- [8] J. Moon, H.-P. Hedman, M. Kemell, A. Tuominen, R. Punkkinen, Hydrogen sensor-of Pd decorated tubular TiO₂ layer prepared by anodization with patterned electrodes on SiO₂ substrate, *Sens. Actuators B: Chem.* 222 (2016) 1990.
- [9] T. Amna, M.S. Hassan, W.S. Shin, H. Van Ba, H.K. Lee, M.-S. Khil, I.H. Hwang, TiO₂ nanorods via one-step electrospinning technique: A novel nanomatrix for mouse myoblasts adhesion and propagation, *Colloids Surf. B: Biointerfaces* 101 (2013) 2224.
- [10] S.J. Chen, H.Y. Yu, B.C. Yang, Bioactive TiO₂ fiber films prepared by electrospinning method, *J. Biomed. Mater. Res. Part A* 101A(1) (2013) 64.
- [11] D. Li, Y.N. Xia, Fabrication of titania nanofibers by electrospinning, *Nano Lett.* 3(4) (2003) 555-560.
- [12] G.M. Kim, S.M. Lee, G.H. Michler, H. Roggendorf, U. Goesele, M. Knez, Nanostructured pure anatase titania tubes replicated from electrospun polymer fiber templates by atomic layer deposition, *Chem. Mater.* 20(9) (2008) 3089-3091.

- [13] R. Chandrasekar, L. Zhang, J.Y. Howe, N.E. Hedin, Y. Zhang, H. Fong, Fabrication and characterization of electrospun titania nanofibers, *J. Mater. Sci.* 44(5) (2009) 1498-505.
- [14] G. Li, J. Liu, G. Jiang, Facile synthesis of spiny mesoporous titania tubes with enhanced photocatalytic activity, *Chem. Commun.* 47(26) (2011) 7443-5.
- [15] G. He, Y. Cai, Y. Zhao, X. Wang, C. Lam, M. Xi, Z. Zhu, H. Fong, Electrospun anatase phase TiO₂ nanofibers with different morphological structures and specific surface areas, *J. Colloid Interface Sci.* 398 (2013) 100-11.
- [16] S. Sanwaria, S. Singh, A. Horechyy, P. Formanek, M. Stamm, R. Srinivasan, Nandan, Fabrication of titania nanostructures using shell polymer nanofibers from block copolymers as templates, *Nanostructures & Nanoobjects* 6 (2016) 1-22.
- [17] A.G. MacDiarmid, W.E. Jones, I.D. Norris, J. Gao, A.T. Johnson, N.J. Pinto, H. Han, F.K. Ko, H. Okuzaki, M. Llaguno, Electrostatically generated nanofibers of electronic polymers, *Synth. Met.* 119(3) (2001) 273-0.
- [18] S.S. Choi, S.G. Lee, S.S. Im, S.H. Kim, Y.L. Joo, Silica nanofibers from electrospinning/sol-gel process, *J. Mater. Sci. Lett.* 22(12) (2003) 899-3.
- [19] S.-H. Lee, C. Tekmen, W.M. Sigmund, Threepoint bending of electrospun TiO₂ nanofibers, *Mater. Sci. Eng. A* 398(1&2) (2005) 7-81.
- [20] W. Nuansing, S. Ninmuang, W. Jarernboon, S. Maensiri, S. Seraphin, *In situ* characterization and morphology of electrospun TiO₂ nanofibers, *Mater. Sci. Eng.* B31(1-3) (2006) 147-155.
- [21] S. Cavaliere, S. Subianto, I. Savych, D.J. Jones, J. Roziere, Electrospinning: designed architectures for energy conversion and storage devices, *Energy Environ. Sci.* 4(12) (2011) 4761-4785.
- [22] G. He, X. Wang, M. Xi, F. Zheng, Z. Zhu, H. Fong, Fabrication and evaluation of dye sensitized solar cells with photoanodes based on electrospun TiO₂ tubes, *Mater. Lett.* 106 (2013) 115-118.

- [23] Y. Wen, B. Liu, W. Zeng, Y. Wang, Plasmonic photocatalysis properties of Au nanoparticles precipitated anatase/rutile mixed TiO_2 nanotubes, *Nanoscale* 5(20) (2013) 9734-9746.
- [24] A. Yousef, N.A.M. Barakat, H.Y. Kim, Electrospun Cd-doped titania nanofiber for photocatalytic hydrolysis of ammonia borane, *Appl. Catal. A: Gen.* 467 (2013) 1098-1108.
- [25] N.A.M. Barakat, E. Ahmed, M.A. Abdelkareem, A.A. Farghali, M.M. Nassar, M.H. El Newehy, S.S. A. Deyab, Ag, Zn and Cd-doped titanium oxide nanofibers as effective photocatalysts for hydrogen extraction from ammonium phosphates, *J. Mol. Catal. A: Chem.* 409 (2015) 117-126.
- [26] A. Nikfarjam, N. Salehifar, Improvement in gas sensing properties of TiO_2 nanofiber sensor by UV irradiation, *Sens. Actuators B* 211 (2015) 146-156.
- [27] C. Peniche, D. Zaldivar, M. Pazos, S. Paz, A. Bulay, J.S. Rocha, Study of the thermal degradation of poly(vinyl-2-pyrrolidone) by thermogravimetry-FTIR, *J. Appl. Polym. Sci.* 50(3) (1993) 485-493.
- [28] W.K. Tang, W.K. Neill, *J. Polym. Sci.* (1964) 65.

Figures and Captions

Figure 1 - SEM images of the as prepared samples obtained by electrospinning of solutions 2 (A), 4 (B), 5 (C) and 7 (D) with TiOSO_4 precursor. Instrumental magnification: 1000X.

Figure 2 - SEM images of the as prepared samples obtained by electrospinning of solutions 2 (A), 3 (B) and 5 (C) with TNBT precursor. Instrumental magnification: 1000X.

Figure 3 - TGA curves obtained with a temperature ramp of 10 °C/min for the samples prepared with solution 7 containing TiOSO_4 precursor (a) and solution 5 containing TNBT precursor (b).

Figure 4 - XRD patterns of TiO_2 (a), TiOSO_x (b), TNBT (c) and TNBT $_x$ (d).

Figure 5 - TEM (A) and HRTEM (B) images of TNBT $_x$. Instrumental magnification: 50000X and 300000X, respectively. Inset C: Fourier Transform of the HRTEM image in (B).

Figure 6 - Fiber diameter distribution (A) and particle size distribution (B) for TNBT $_x$ sample. (n.f. = number of fibers; n.p. = number of particles).

Figure 7 - HR-TEM image of the TNBT sample before thermal treatment. Instrumental magnification: 250000X.

Figure 8 - SEM image of the as prepared sample obtained by electro spray of solution 5 with TNBT precursor and PVP of 30000 units. Instrumental magnification: 5000X.

Figure 9 - XRD patterns of the TiO_2 samples obtained by electro spray (a) and by solvent evaporation (b).

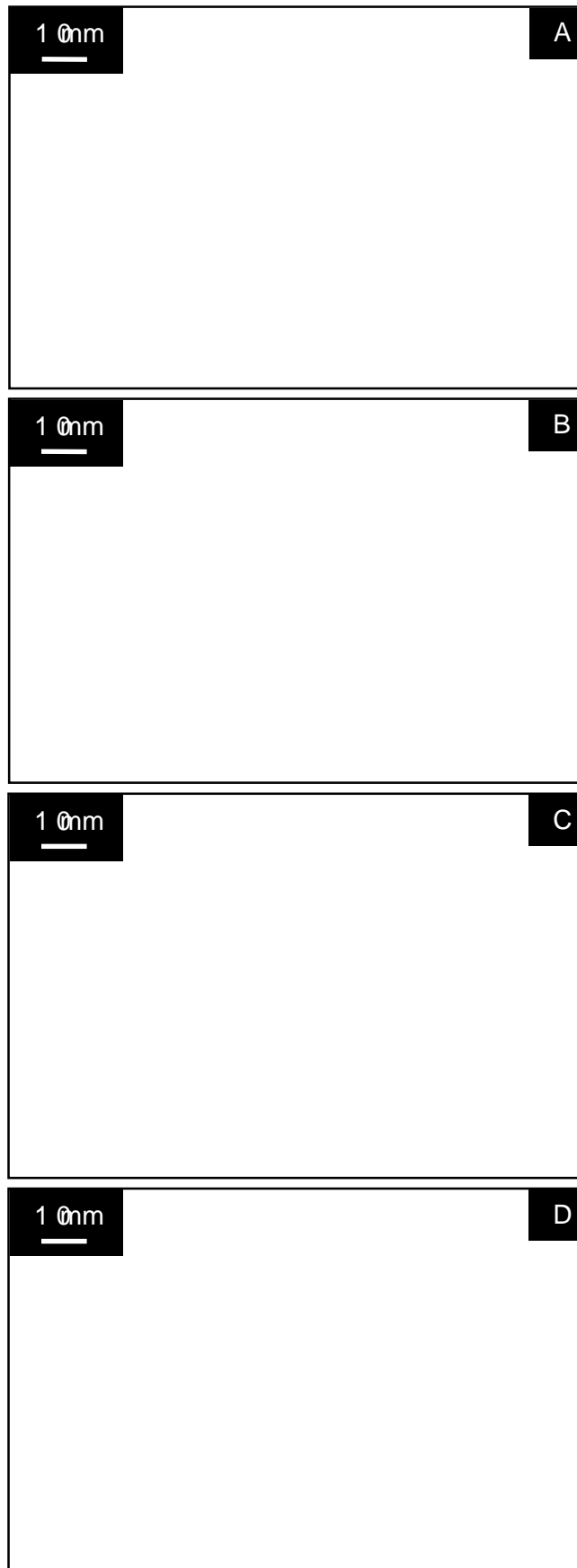


Figure 1

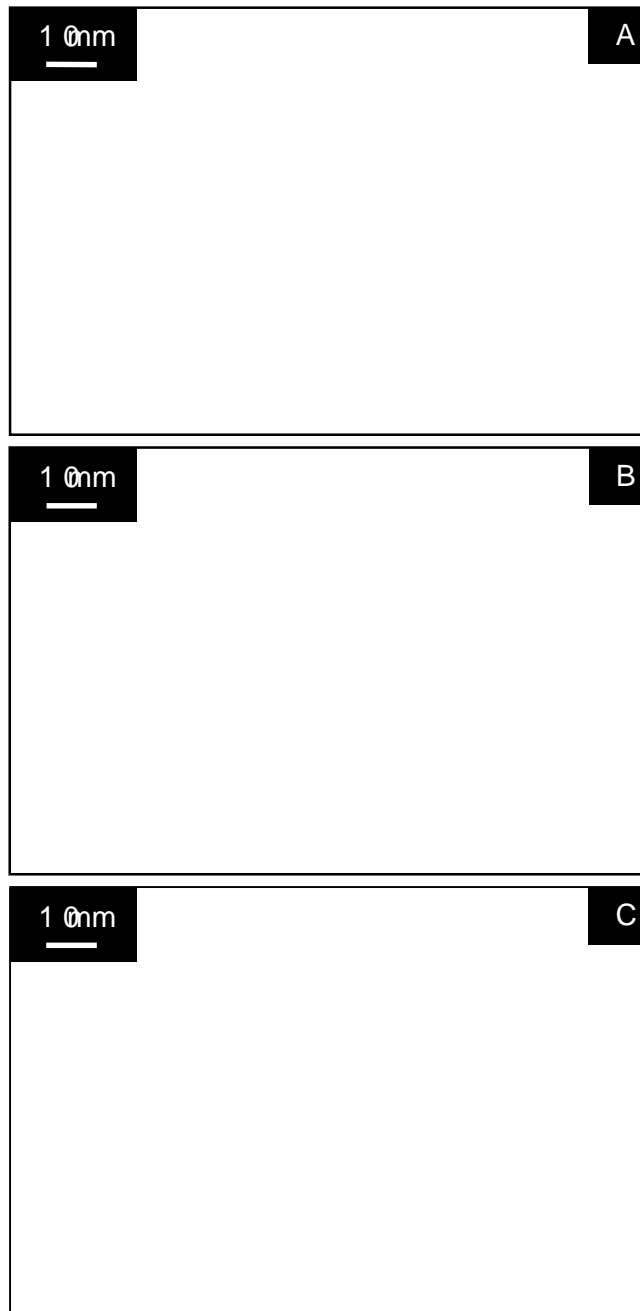


Figure 2

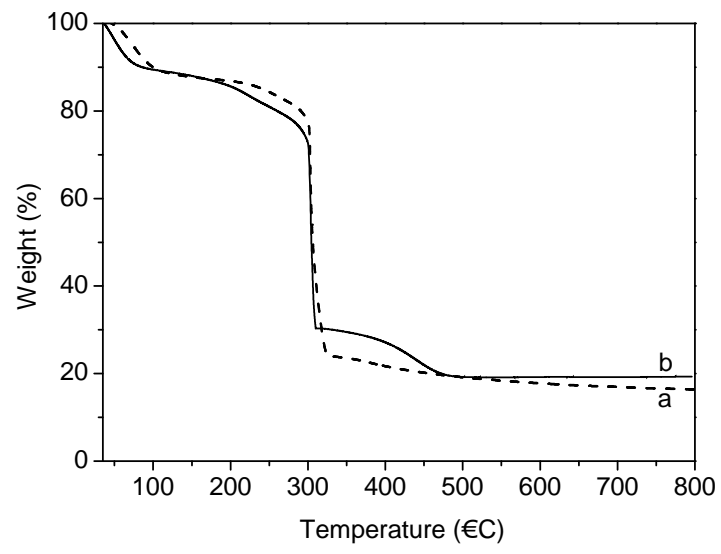


Figure 3

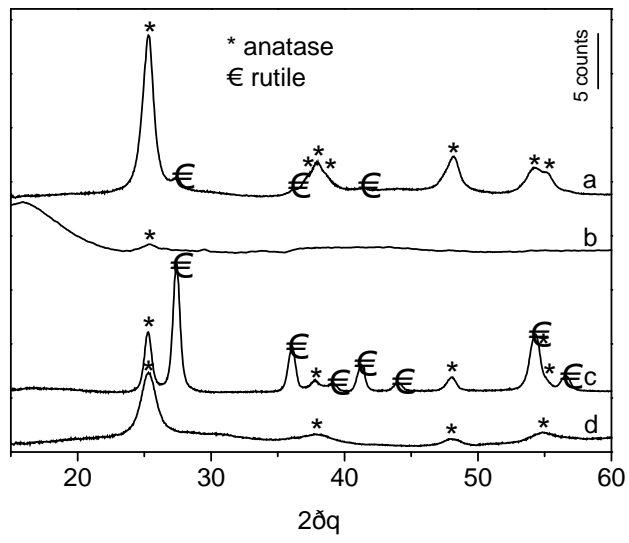


Figure4

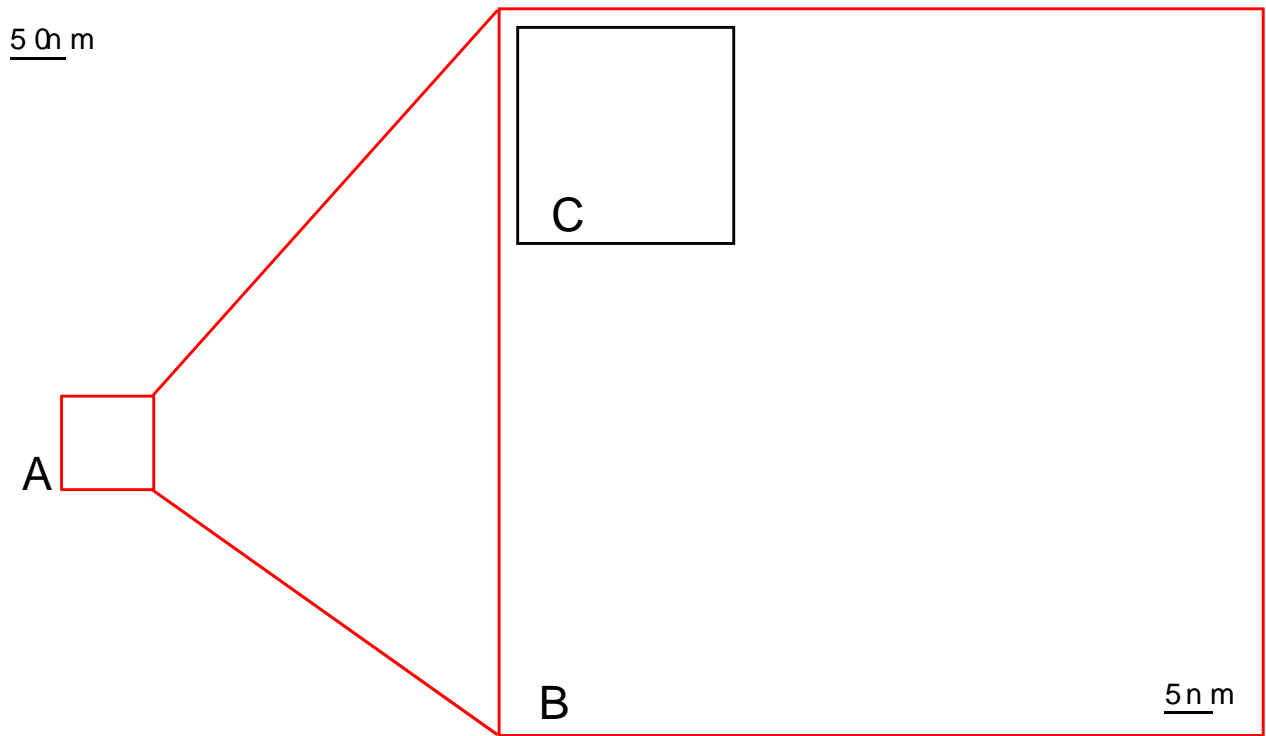


Figure5

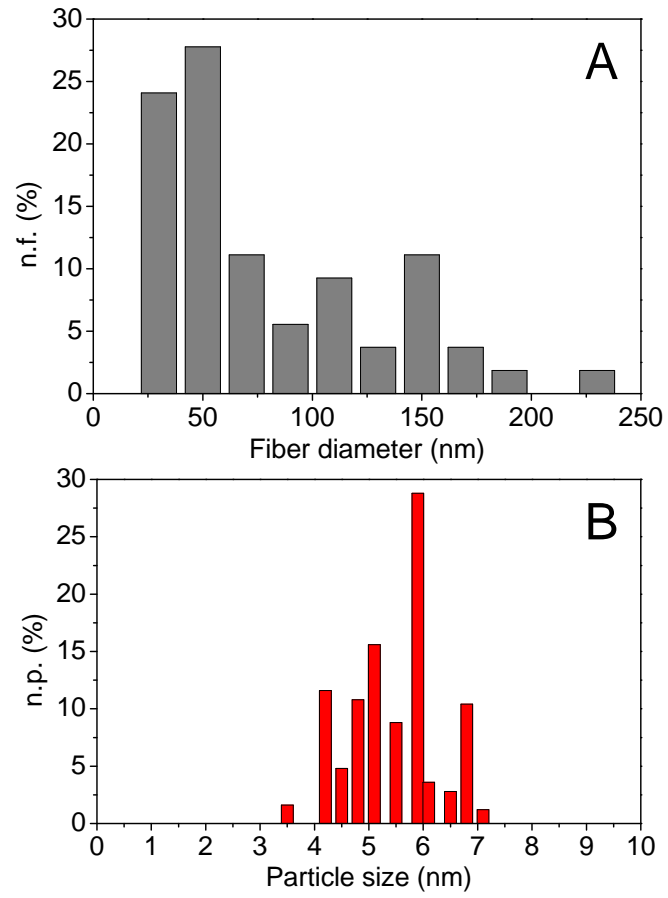


Figure 6



1.0 m

Figure7

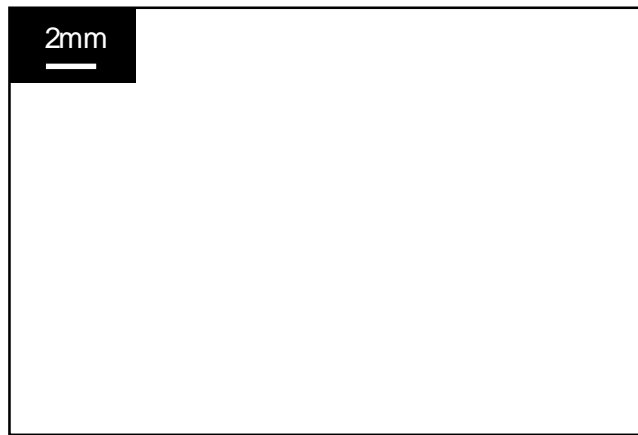


Figure8

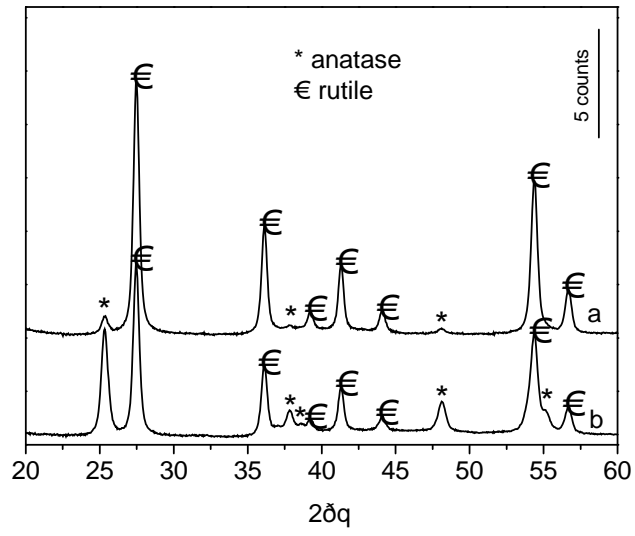


Figure9